Manipulation of modified clay particles in a nematic solvent by a magnetic field

2007 J. Phys.: Condens. Matter 19 156103

(http://iopscience.iop.org/0953-8984/19/15/156103)

IOP PUBLISHING JOURNAL OF PHYSICS: CONDENSED MATTER

J. Phys.: Condens. Matter **19** (2007) 156103 (17pp) doi:10.1088/0953-8984/19/15/156103

Manipulation of modified clay particles in a nematic solvent by a magnetic field

Joan Connolly[1], Jeroen S van Duijneveldt[2], Susanne Klein[3], Claire Pizzey[2,4] and Robert M Richardson[1]

[1] H H Wills Laboratory, University of Bristol, Tyndall Avenue, Bristol BS8 1TL, UK
[2] School of Chemistry, University of Bristol, Cantock's Close, Bristol BS8 1TS, UK
[3] HP Laboratories, Filton Road, Stoke Gifford, Bristol BS34 8QZ, UK

Received 2 October 2006, in final form 12 January 2007
Published 26 March 2007
Online at stacks.iop.org/JPhysCM/19/156103

Abstract

The magnetic alignment of organically modified montmorillonite platelets in magnetic fields is studied using small-angle x-ray scattering. When suspended in non-mesogenic solvents such as dodecanol the platelets are found to align parallel to the magnetic field due to the negative anisotropy of the magnetic susceptibility of the montmorillonite. Alignment of the clay in the nematic phase of 5CB was possible for sufficiently dilute samples and at sufficiently high field strengths. However, in this case the platelets aligned with their normals parallel to the field. It is argued that this is due to homeotropic anchoring of the liquid crystal at the clay particle surfaces leading to the particle orientation being slaved to the director alignment. Alignment of the 5CB director parallel to the field was only apparent at high fields and low particle concentrations, where the magnetic coherence length of the liquid crystal would be smaller than the typical size of a domain between stacks of clay platelets. A simple theoretical model is presented to aid the interpretation of the observations. The observed degree of particle alignment is often less than predicted, probably as the result of interactions between stacks of particles opposing reorientation.

1. Introduction

When using liquid crystals as the solvent for suspending colloidal particles, the interplay of surface alignment and elastic energies gives rise to a wealth of phenomena [1]. The most thoroughly studied systems consist of spheres in the size range of 0.5–10 μm suspended in nematic solvents. These systems show various different defects that are easily studied under the polarization microscope [2] and allow confirmation of the behaviour of the liquid crystal director predicted by theoretical modelling [1]. The observed Saturn ring, dipole and surface ring defects are typical for the topological constraints of homeotropically anchored liquid

[4] Present address: Chemical and Biological Engineering, University of Wisconsin-Madison, 1415 Engineering Drive, Madison, WI 53703, USA.

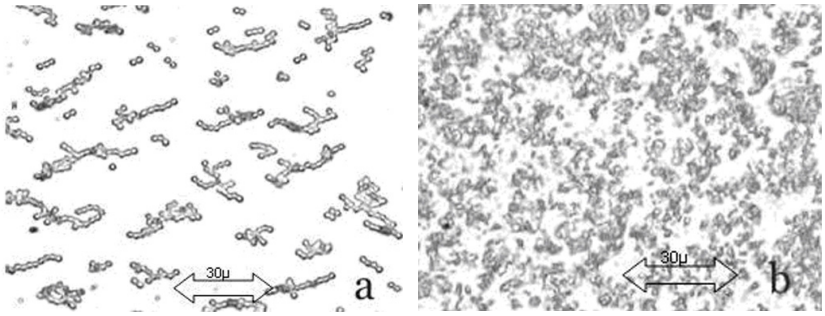

Figure 1. Both 5CB suspensions contain 1% w/w of particles. The substrates were coated with a planar alignment layer to suppress domain formation. The substrate separation was 10 μm. (a) The particles are polymer spheres with a mean diameter of 2 μm. Chain formation and the beginning of 'pocket' formation are clearly visible. (b) 1% w/w of Claytone AF forms an open floc in 5CB.

crystal molecules on a sphere. The interaction between the solvent and the suspended spheres leads to defect stabilized gel and glass formation [3]. The gels can be switched by an electric field between clear and scattering and show some bi-stable behaviour, i.e. they remain in the same optical state when the switching voltage is taken off [4]. This holds true for non-spherical particles as well [5].

Suspensions of spheres and anisometric particles share the feature of a memory effect but differ in many other aspects. For montmorillonite platelets aggregation occurs as for spheres but the structure formed looks quite different when examined under the polarization microscope (see figure 1). The suspension can again be switched between clear and scattering [5]. In the cases of a network formed by spheres or a polymer dispersed nematic the switching is based on reorientation of the liquid crystal only. In the pockets formed by the network of spheres or the polymer the director is homeotropically aligned at the surface of the pocket. This leads to an index mismatch between neighbouring droplets. When a field is applied the liquid crystal orients parallel to the field lines. The index mismatch between neighbouring droplets disappears and the sample turns transparent. In our case, that is asymmetric particles in a nematic matrix, it was not clear whether index matching was achieved by reorientation of the liquid crystal only or whether the particles were rotated as well.

The dimensions of the platelets used (thickness of 1 nm and typical diameter 500 nm) do not allow direct observation by optical means. Small angle x-ray scattering (SAXS) revealed that the suspension consists of a mixture of single platelets and stacks with solvent dependent inter-platelet spacings [6]. The number of platelets in stacks and the number of free plates also depends on the solvent. In toluene for example we found for organically modified montmorillonite that about 80% of all particles are single platelets, whereas in the liquid crystal 5CB 80% of all particles are organized in stacks of on average four to five platelets. In addition, there is a marked tendency for the single platelets and stacks to assemble into larger scale aggregates [7].

Electron spin resonance (ESR) studies have established that the alignment of the nematic director within a magnetic field is influenced by the dispersed platelets [8]. Below 3% w/w particle concentration the director will follow the applied field of 0.3 T. Above this concentration the director is pinned into random orientation by the surface alignment of the platelets [8]. However, ESR experiments only probe the behaviour of the solvent liquid crystal and not that of the colloidal particles.

In this paper we report a detailed investigation of the degree of alignment and ordering within the liquid crystal/clay composites. We chose a organic solvent/clay system because

its switching behaviour mentioned above leads to potential applications in displays [9]. The orientational distribution of the clay platelets has been studied using SAXS from suspensions in magnetic fields. We have focussed on one system with a nematic solvent, 5CB, but we also report results from the same clay in a non-mesogenic solvent in order to characterize the behaviour of the clay on its own in an applied field.

2. Experimental details

2.1. Samples

In this study we used a commercially available organophilic clay, Claytone AF (Rockwood Additives). The clay mineral is montmorillonite, which has a primary platelet thickness of 1 nm. Furthermore, the platelets have a tendency to form stacks consisting of a number of platelets. Scanning electron microscopy showed that the platelets had a broad distribution of diameters, with a typical diameter around 500 nm. The surface is treated with dihydrogenated tallow, a polydisperse surfactant mixture, the major component of which is dimethyldioctadecylammonium bromide (DODAB). The low molecular weight surfactant stabilizes the particles against mutual attractive forces in order to suspend the particles within the nematic matrix and reduce subsequent aggregation. Excess surfactant was removed by washing the clay in a 40/60 mixture of propanol and water (ultra-pure, Millipore). The clay was then dried under vacuum to remove any excess water and ground using a mortar and pestle to aid dispersion.

As solvents we chose one liquid crystal and a non-mesogenic solvent. The liquid crystal was 5CB (K15, Merck, used as received). It is a single-component liquid crystal with a nematic/isotropic transition temperature of 35 °C, which stayed unchanged on addition of the clay [10, 11]. The non-mesogenic solvent was dodecanol (Sigma-Aldrich, used as received). In [7] we showed that different suspension preparation methods yielded similar degrees of delamination and stack sizes. Samples were generally prepared by adding the dried clay in powder form to the solvent in its isotropic state and stirring for 15 min. The suspensions were transferred to an ultrasonic bath (Fisherbrand FB11020 with an operating power of 100 W emitted through two transducers located in the base) and sonicated for 6–7 h. This was found to be a convenient method of preparation. Other methods gave the same results [7]. The samples were stable, i.e. no sedimentation was visible over the course of the experiments.

2.2. Small angle x-ray scattering

The scattering from suspensions of Claytone AF in 5CB or dodecanol has been measured using three different small angle x-ray scattering cameras. In all three cases the layout was the same and is illustrated schematically in figure 2. A monochromatic x-ray beam is incident on the temperature controlled sample and the scattering pattern is recorded on a two-dimensional detector. A variable magnetic field is applied perpendicular to the beam. The scattering at different azimuthal angles, ϕ (see figure 2), corresponds to different orientations of the scattering vector, **Q**, with respect to the field. For $\phi = 0°$ the scattering vector is approximately parallel to the field, and for $\phi = 90°$ it is perpendicular. The details of the experimental arrangements are as follows.

The first set of experiments was done using the BM02 [12] station at the European Synchrotron Radiation Facility, Grenoble. A wavelength of 1.08 Å was used and the two-dimensional CCD detector was positioned to give a Q range of 0.013–0.40 $Å^{-1}$. In this case the magnetic field was provided by a pair of permanent magnets either side of the sample. The

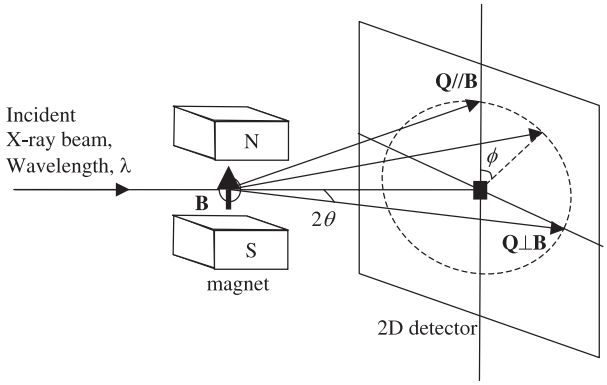

Figure 2. The geometry of a scattering experiment from samples with applied magnetic field.

pole gap could be adjusted to vary the magnetic field, which had been previously calibrated by ESRF staff. The maximum field was 0.84 T. The samples were contained in 1.5 mm diameter Lindemann glass tubes and their temperature was controlled by a thermostatted jet of nitrogen gas.

The second set of experiments was done using station 2.1 at the Daresbury Synchrotron Radiation Source [13]. A wavelength of 1.5 Å is standard on this instrument and the two-dimensional multiwire detector was positioned to give a Q range of 0.032–0.37 Å^{-1}. The magnetic field was provided by an electromagnet. The field could be varied by changing the current and it had been previously calibrated using a Hall probe. A maximum field of 1.26 T was applied. The samples were contained in 2 mm Lindemann glass tubes that had been flattened to give a path length of about 1 mm through the scattering material. The sample was placed in an aluminium block whose temperature was maintained by cartridge heaters and a type K thermocouple connected to a Eurotherm controller.

The third set of experiments was done using SAXS apparatus [10] at Bristol. This apparatus is similar to station 2.1 but the beam is provided from a sealed tube and a graphite monochromator. For these experiments the sample was aligned outside the beam using a 4.5 T NMR magnet and the scattering was measured with no field applied.

2.3. Data analysis

Figure 3(a) shows typical scattering data from a suspension of Claytone in 5CB. Figure 3(b) shows the data regrouped to give the intensity of the pseudo-Bragg peak from the clay versus the azimuthal angle.

In this paper, we use the scattering data to characterize the alignment of the different constituents in the suspension in terms of order parameters. The orientational order parameter of the platelets is defined by the distribution of platelet surface normals, $f(\beta)$, where β is the angle between a normal and the applied field.

$$\overline{P_{2\,\text{CLAY}}} = \int f(\beta)\left(\tfrac{3}{2}\cos^2\beta - \tfrac{1}{2}\right)\mathrm{d}\cos\beta. \tag{1}$$

The orientational order parameter of the 5CB director (not the molecular order parameter) is similarly defined by the distribution of the director, $g(\gamma)$, where γ is the angle between the director and the applied field

$$\overline{P_{2\,\text{DIRECTOR}}} = \int g(\gamma)\left(\tfrac{3}{2}\cos^2\gamma - \tfrac{1}{2}\right)\mathrm{d}\cos\gamma. \tag{2}$$

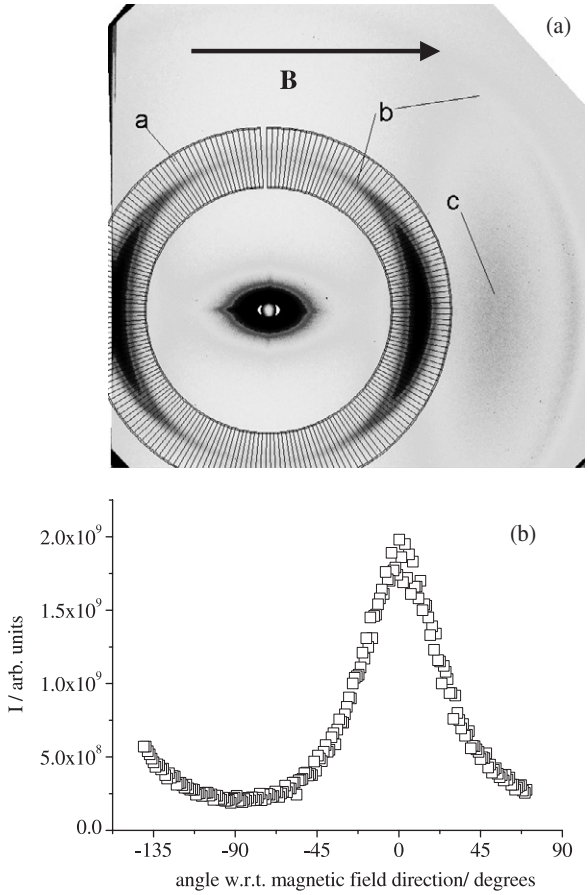

Figure 3. (a) SAXS pattern from 1% w/w Claytone in 5CB: a, arcs defining regions for extracting orientational distribution; b, Claytone scattering peak; c, 5CB scattering peak. (b) Intensity of Claytone peak with angle from the magnetic field direction. Each point on the plot corresponds to the intensity of one of the arcs shown in (a).

The main features of the scattering are pseudo-Bragg peaks at $Q = 0.17$ and 0.34 Å^{-1} from stacks of Claytone platelets and a diffuse peak at $Q = 0.26$ Å^{-1} that originates from the end to end correlation of the molecules in 5CB [14]. The Claytone pseudo-Bragg peaks are part of a continuous curve that shows a power law dependence at low Q, resulting from large open aggregates of platelet stacks with some single platelets. Since most of the Claytone platelets are in the stacks (>80%), we have used the azimuthal distribution of the first order pseudo-Bragg peak from Claytone to estimate their orientational order.

We have regarded the platelets as nearly rigid because they generally appear to be flat in electron microscope images and an estimate of the thermally activated bend is very low. The thermally activated bend (expressed as the root mean square (rms) angle δ of the platelet normal with respect to its mean) may be roughly estimated by equating the bending energy to mean thermal energy ($\frac{1}{2}k_{\mathrm{B}}T$), which leads to the equation

$$\delta_{\mathrm{RMS}} \approx \sqrt{\frac{k_{\mathrm{B}}T}{Yh^3}} \tag{3}$$

where Y is Young's modulus for a single platelet and h is its thickness. Since the Young's modulus is about 200 GPa [15, 16], the value δ_{RMS} arising from the flexibility of the sheets is 0.3°, which is negligible.

The inter-plate vector of a Claytone stack is perpendicular to the platelets and, since the plates are nearly rigid, the angular distribution of the pseudo-Bragg peak on the detector reflects the distribution of platelet normals. The intrinsic azimuthal spread of the diffraction peak from a perfectly aligned stack of 0.5 μm diameter discs is very small ($\Delta Q \sim 1.2 \times 10^{-3}$ Å^{-1}) so the only significant contribution to the transverse width of the peak is the distribution of orientations. The orientational order parameter for the clay platelets may be calculated by dividing the intensity from the first order peak from the clay into N arcs and using the equation

$$\overline{P_{2\,\mathrm{CLAY}}} = \frac{\sum_{i=1}^{N}\left(\left(\frac{3}{2}\cos^2\phi_i - \frac{1}{2}\right) I_{\mathrm{clay}}(\phi_i)\sin\phi_i\right)}{\sum_{i=1}^{N}\left(I_{\mathrm{clay}}(\phi_i)\sin\phi_i\right)}. \tag{4}$$

The values of $I_{\mathrm{clay}}(\phi_i)$ were determined by summing up the diffracted intensity in each box and subtracting background interpolated from detector pixels just inside and just outside the band.

The diffuse 5CB peak from end-to-end correlations of the molecules lies on the director in reciprocal space and so can be used to estimate the orientational order of the director. The peak has a significant intrinsic transverse width because the smectic-like order in the nematic has a very short range. Thus there would be an intrinsic transverse spread even if the director were perfectly aligned. The ordering of the 5CB director has been quantified using a similar approach to the clay but the values obtained for the director order parameter will be low because of the intrinsic peak width.

$$\overline{P_{2\,\mathrm{DIRECTOR\_OBSERVED}}} = \frac{\sum_{i=1}^{N}\left(\left(\frac{3}{2}\cos^2\phi_i - \frac{1}{2}\right) I_{5\mathrm{CB}}(\phi_i)\sin\phi_i\right)}{\sum_{i=1}^{N}\left(I_{5\mathrm{CB}}(\phi_i)\sin\phi_i\right)}. \tag{5}$$

It can be shown by using the spherical harmonic addition theorem [17] and invoking the cylindrical symmetry of the phase [18] that the true order parameter of the director may be related to that measured from the scattering by the equation

$$\overline{P_{2\,\mathrm{DIRECTOR\_OBSERVED}}} = \overline{P_{2\,\mathrm{DIRECTOR\_TRUE}}} \times \overline{P_{2\,\mathrm{INTRINSIC}}} \tag{6}$$

where $\overline{P_{2\,\mathrm{INTRINSIC}}}$ refers to the value that would be obtained from the scattering from a perfectly ordered system (with $\overline{P_{2\,\mathrm{DIRECTOR\_TRUE}}} = 1$). We have not attempted to make this conversion but have simply used $\overline{P_{2\,\mathrm{DIRECTOR\_OBSERVED}}}$ as an empirical measure of the alignment of the director.

3. Results

3.1. SAXS results on alignment of Claytone in non-mesogenic solvents

It was found that suspensions of Claytone in several non-mesogenic solvents gave anisotropic scattering patterns when a magnetic field was applied. Figure 4 shows the scattering from a suspension of Claytone in dodecanol with and without the field applied.

Under the influence of the field, the pseudo-Bragg peaks align in a direction perpendicular to the magnetic field, indicating that the platelets lie approximately parallel to the field. When the field is removed, the scattering becomes isotropic again. Figure 5 shows the orientational order parameters for a 1% suspension of Claytone in dodecanol as a function of applied field. The order parameters are negative because the platelet normals are oriented roughly perpendicular to the field. If this alignment were perfect, a value of −0.5 would be reached.

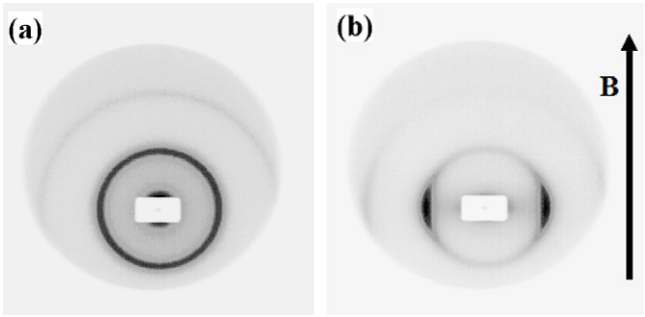

Figure 4. SAXS patterns from Claytone in dodecanol with (a) zero applied field and (b) 1.2 T applied field. The peaks on the plot are pseudo-Bragg peaks from the regular Claytone platelets. The magnetic field induces alignment of the Claytone stacks.

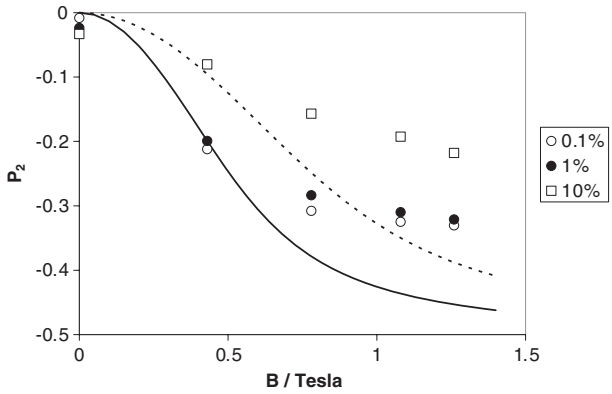

Figure 5. The points show the orientational order parameter for the clay platelets $\overline{P_{2\,\mathrm{CLAY}}}$ in 0.1%, 1% and 10% suspensions in dodecanol. The lines are the fits of equation (15) to the 1% data. The solid line is fitted to the low B value only.

3.2. SAXS results: the alignment of Claytone in 5CB

We have found that a sufficiently strong magnetic field always tends to align clay platelets in a 5CB suspension with their normals parallel to the field. This is different from the behaviour observed for dodecanol (or octanol and other non-mesogenic solvents). The exact magnitude of the field required to align the clay platelets in 5CB is not easy to reproduce. It is sensitive to the size and geometry of the sample container and to the sample batch. We also found that flow alignment of the clay stacks sometimes occurred when the suspensions were injected through a syringe needle into the capillaries used in the SAXS experiments. This flow alignment disappeared in the isotropic phase. In order to obtain reproducible alignment observations it was necessary to cool samples into the nematic phase from the isotropic phase in the magnetic field. Below we focus on observations made in this way.

Typical SAXS data from an aligned sample of Claytone in 5CB are shown in figure 3(a). The result was obtained using a field of 0.84 T applied to a sample in a 1.5 mm diameter circular cross-section capillary, whereas 1.26 T was unable to align the clay in a flattened tube of around 1 mm thickness. Figure 6 shows an example where the clay has not aligned although the azimuthal distributions of the two peaks show that the 5CB has aligned. The clay alignment is only observed when the clay–5CB suspension is cooled from isotropic to nematic (I $\rightarrow$ N)

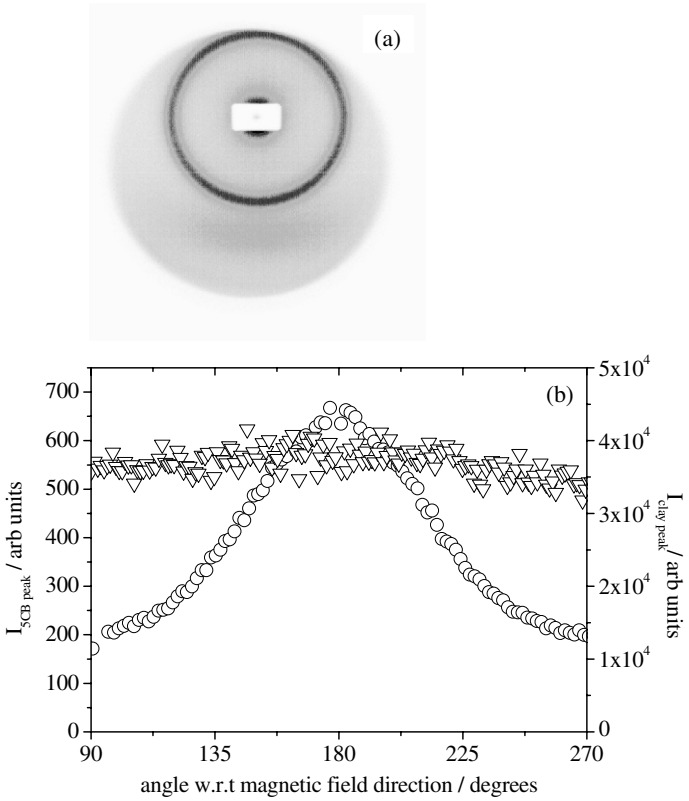

Figure 6. SAXS results of 1% Claytone in 5CB at Daresbury. (a) The image appears to show alignment of the clay and 5CB, but (b) analysis reveals that while the 5CB (circles) is aligned the clay (triangles) is not.

Table 1. Effect of field and concentration on $\overline{P_{2\,\mathrm{CLAY}}}$ for clay in 5CB suspensions in 1.5 mm tubes.

Experimental conditions	Concentration (%)	$\overline{P_{2\,\mathrm{CLAY}}}$
∼1 T, I → N in field	0.1	0.26
	1	0.30
4.5 T, I → N in field	1	0.35
	10	0.20
4.5 T applied in isotropic then I → N in zero field	10	0.08

in a magnetic field. Cooling in zero field and then applying a field to the nematic does not align the stacks of clay plates. Comparing the clay alignment in 5CB shown in figure 3 with that shown in non-mesogenic solvents such as dodecanol (e.g. figure 4) shows that the liquid crystal is influencing the direction of alignment of the clay stacks.

In 5CB, the stacks tend to be aligned with their normals parallel to the field and the degree of this order may be quantified using the order parameter described in the data analysis section. Table 1 shows the results for alignment in comparable experimental conditions (1.5 mm cylindrical tubes). As the concentration of clay increases, higher fields are necessary to align the clay in the samples with a ∼1 T field aligning the clay plates in a 1% w/w or less concentrated

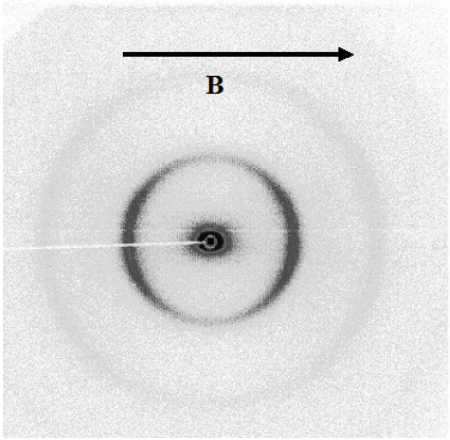

Figure 7. SAXS pattern of 10% w/w Claytone in 5CB after cooling from nematic in a 4.5 T field. The clay stacks show alignment even though no 5CB peak is detectable.

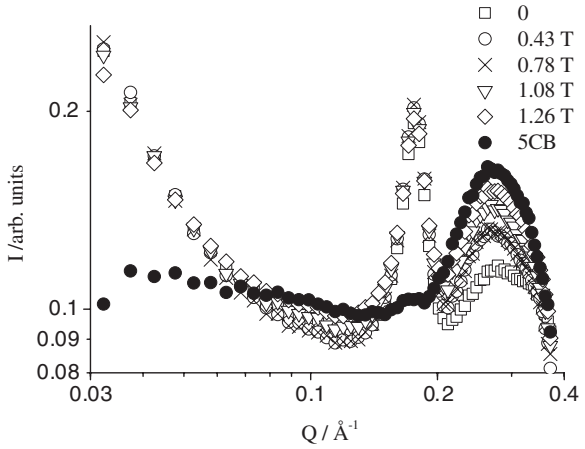

Figure 8. The intensity of the 5CB peak increases with field for 0.2% Claytone in 5CB. The open symbols are the scattering from a 0.2% w/w Claytone in 5CB suspension. The closed circles are the scattering from pure 5CB.

suspension but a 4.5 T field needed to align a 10% w/w suspension as shown in figure 7. No significant alignment of the clay was found when the magnetic field was applied in the isotropic phase.

In suspensions of Claytone in nematic 5CB, the diffuse peak from the 5CB is expected at $Q \sim 0.26$ Å^{-1}. Figure 8 shows the regrouped intensity from a 0.2% suspension with various magnetic fields applied to a sample where no alignment of the clay occurred. For zero field the 5CB peak is barely visible, but as the aligning field is increased the peak becomes stronger. This suggests that the unaligned clay has randomized the director so the diffuse peak is spread over the surface of a sphere in reciprocal space. The application of the field re-orientates the director so that the diffuse peak lies on the Ewald sphere and its scattering is observed.

This interpretation is supported by the influence of the clay concentration on the intensity of the diffuse 5CB peak. This can be seen in figure 9 where the 5CB peak at $Q = 0.26$ Å^{-1} is suppressed as the concentration of clay increases. Figure 10 shows this effect more

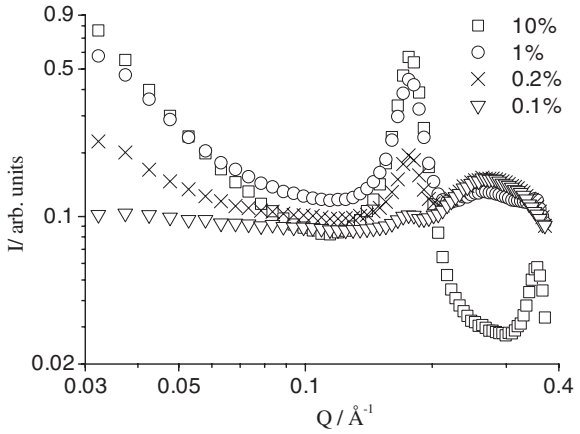

Figure 9. Scattering intensity for various concentrations of Claytone in 5CB in a magnetic field.

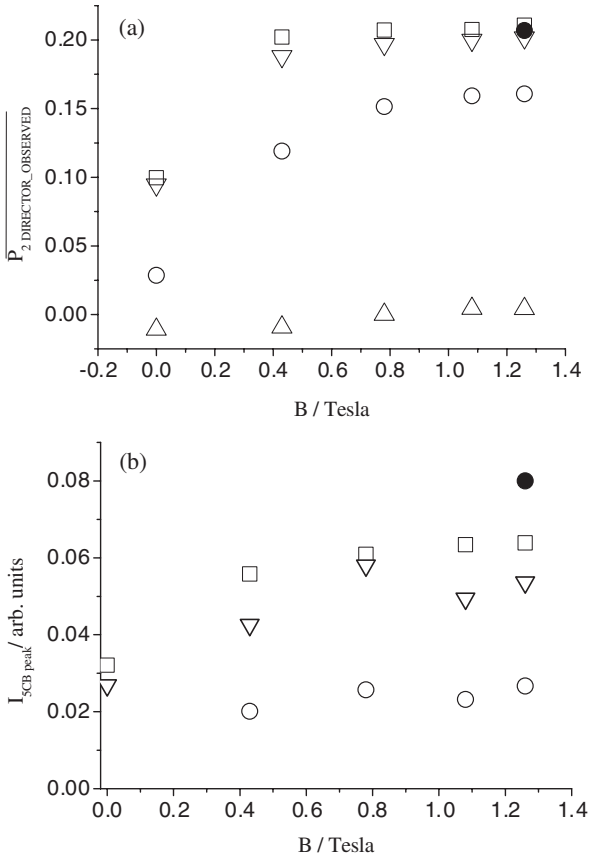

Figure 10. Effect of the magnetic field strength on (a) $\overline{P_{2\,\mathrm{DIRECTOR\_OBSERVED}}}$ and (b) intensity of the 5CB peak for 10% w/w (triangles), 1% w/w (circles), 0.2% w/w (inverted trianges) and 0.1% w/w (squares) suspensions of Claytone AF in 5CB and pure 5CB (filled circle).

quantitatively for a set of samples where the alignment of the clay was negligible. Figure 10(b) shows that the 5CB peak (corrected for background from the clay) increases as the magnetic field increases but the increase is much weaker for the higher concentration. The increased alignment of the 5CB with field is not due to a change in clay content, as a result of settling for instance, since the intensity of the clay stack peak is constant for all fields.

Figure 10(a) summarizes the 5CB alignment behaviour. The increase in the $\overline{P_{2\,\mathrm{DIRECTOR\_OBSERVED}}}$ value with field mirrors the changes in the magnitude of the peak intensity with field. The lower concentration suspensions have a $\overline{P_{2\,\mathrm{DIRECTOR\_OBSERVED}}}$ close to that of the pure 5CB, while the 1% suspension increases with field but is 75% of the pure value at 1.2 T. The 10% suspensions show no 5CB alignment and hence no measurable $\overline{P_{2\,\mathrm{DIRECTOR\_OBSERVED}}}$. It is interesting to note that although the director order parameter of the most dilute (0.1%) suspension approaches that of pure 5CB the intensity is significantly lower in the clay–5CB suspensions. This suggests that there are regions of 5CB with random director orientations remaining even at fields of 1.4 T.

Figure 7 shows a scattering pattern recorded with zero applied field from a 10% w/w clay suspension cooled from isotropic in a 4.5 T field. The pattern does not show any 5CB peak despite the partial alignment of the clay stacks in the suspensions. Since the clay alignment is opposite to that expected for clay in a non-mesogenic solvent, the 5CB must still be exerting an aligning torque on the platelets even though its director is not significantly aligned parallel to the field. However, the NMR spectrum of the 10% w/w clay suspension in a 7 T field shows the typical peaks for the nematic phase of pure 5CB, indicating the director was parallel to the field [19]. We return to this peculiar result below.

4. Discussion

There are two striking features in the results described above. First, a magnetic field induces opposite alignment of clay platelets in nematic and non-mesogenic solvents. Second, the alignment of the 5CB director parallel to the field is only apparent at high fields and low concentrations. In the section below a simple model is constructed to rationalize these and other observations.

4.1. Orientation dependent energy of a suspended clay platelet

A rigid clay particle, that is either a single platelet or a stack of platelets, whose normal is at an angle β to an applied field B, is shown in figure 11. The boundary conditions are homeotropic so the director is strongly anchored perpendicular to the clay surface. At distances remote from the clay platelet the director becomes parallel to the field to minimize the magnetic energy density (assuming that the liquid crystal has a positive anisotropy of the magnetic susceptibility $\Delta\chi_{\mathrm{L}}$, as is the case here).

We assume that the director orientation decays with a characteristic length, ξ, as

$$\sin\gamma = \sin\beta\exp(-z/\xi) \tag{7}$$

where z is the distance from the platelet [20]. The magnetic free energy density at any point depends upon the angle between the director and the field and $\Delta\chi_{\mathrm{L}}$ of the solvent.

$$u_{\mathrm{M}}(z) = \frac{\Delta\chi_{\mathrm{L}}B^2}{2\mu_0}\sin^2\beta = \frac{\Delta\chi_{\mathrm{L}}B^2}{2\mu_0}\sin^2\beta\exp(-2z/\xi) \tag{8}$$

where μ_0 is the permeability of free space.

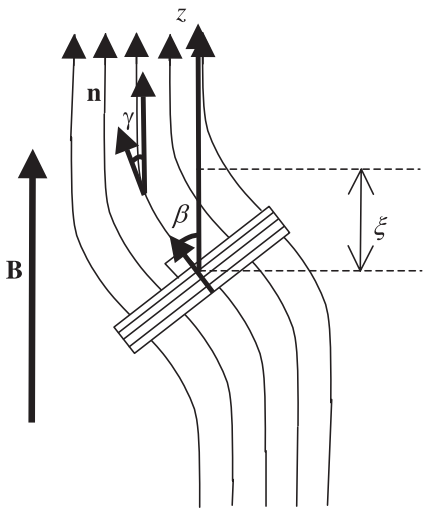

Figure 11. Showing stack of platelets oriented with respect to applied field, B, and schematic bending of the director, n. The deviation angles of the platelet normal, β, and the director, γ, are shown.

The elastic free energy at any point depends on the bend of the director at that point and the bend elastic constant, K_3.

$$u_{\mathrm{E}}(z) = \frac{K_3}{2}\left(\frac{\partial \sin\gamma}{\partial z}\right)^2 = \frac{K_3}{2}\sin^2\beta\frac{1}{\xi^2}\exp(-2z/\xi). \tag{9}$$

To calculate the total orientational free energy of the liquid crystal, it is necessary to sum these two contributions and integrate over a volume large enough to include the entire region in which the director deviates from the field. We ignore other possible contributions such as defect energies and edge effects as they are of secondary importance for large flat platelets. The integration of the exponential over z gives a factor of ξ and the integration over the other two coordinates will give a factor of approximately A, the platelet area. Hence the orientational free energy in the (nematic) solvent around one platelet, U_{L}, is given by

$$U_{\mathrm{L}} \approx \frac{A}{2}\sin^2\beta\left[\frac{\Delta\chi_{\mathrm{L}}B^2}{\mu_0} + \frac{K_3}{\xi^2}\right]\xi. \tag{10}$$

The characteristic distance, ξ, results from a balance between the magnetic and elastic influences on the director and is known as the magnetic coherence length. It is an inverse function of the applied field [20]:

$$\xi = \frac{\mu_0}{B}\sqrt{\frac{K_3}{\Delta\chi_{\mathrm{L}}}}. \tag{11}$$

In a dispersion of many stacks of platelets there may be a typical spacing between stacks, d. It is interesting to note in passing that if $\xi \ll d$ then most of the nematic will be aligned with its director parallel to the field. If $\xi \gg d$ then the directors will be distributed according to the orientations of the platelet normals. Combining the above two equations shows that the orientational free energy in the (nematic) solvent U_{L} around one platelet is linear in the field and not proportional to its square as might be presumed from equation (8).

$$U_{\mathrm{L}} = A\sin^2\beta_0\sqrt{\frac{\Delta\chi_{\mathrm{L}}K_3}{\mu_0}}B. \tag{12}$$

Assuming there is no permanent magnetic moment on a platelet, the orientational part of its free energy may be calculated from the volume, V, of the particle, that is either a single platelet or a stack, and the anisotropy of the susceptibility, $\Delta\chi_C$, of the platelet material,

$$U_C = \frac{V\Delta\chi_C B^2}{2\mu_0}\sin^2\beta. \tag{13}$$

So the total orientational free energy of a platelet and its surroundings, $U = U_L + U_C$, is given by

$$U(\beta) = \sin^2\beta\left[A\sqrt{\frac{\Delta\chi_L K_3}{\mu_0}}B + \frac{V\Delta\chi_C}{2\mu_0}B^2\right]. \tag{14}$$

If $\Delta\chi_C$ is negative, it is possible that the sign of $U(\beta)$ may reverse as the field increases. At low fields platelet normals parallel to the field would be favoured because the liquid crystal director is aligned and the elastic energy penalty of rotating the platelet normal away from the field is large. At large fields, in this case more than 14 T (see below), the elastic energy becomes less significant than the magnetic energy of the particle and so the platelet normals perpendicular to the field would be favoured. The data reported here does not show this high field behaviour for the nematic solvent although it does show this behaviour in the non-mesogenic solvent. This expression is applicable to nematic solvents with homeotropic boundary conditions at the platelet. It is also applicable to non-mesogenic solvents with the first term in the brackets set to zero (since $K_3 = 0$ and $\Delta\chi_L = 0$):

$$U(\beta) = \sin^2\beta\frac{V\Delta\chi_C}{2\mu_0}B^2. \tag{15}$$

If other contributions to the orientational free energy such as inter-stack interactions are negligible, the platelet normal distribution, $f(\beta)$, can be calculated

$$f(\beta) \propto \exp\left(\frac{-U(\beta)}{k_B T}\right)$$

where k_B is Boltzmann's constant and T is the temperature. Hence the order parameter, $\overline{P_{2\,\mathrm{CLAY}}}$, may be calculated using equation (1). If U increases as β increases, the platelet normals prefer to lie parallel to the field and a positive value of $\overline{P_{2\,\mathrm{CLAY}}}$ results. If U decreases as β increases, the platelet normals prefer to lie perpendicular to the field and a negative value of $\overline{P_{2\,\mathrm{CLAY}}}$ results.

4.2. Analysis of order parameters for clay in dodecanol

In the clay in dodecanol suspensions the magnetically induced alignment must be caused by the anisotropy of the magnetic susceptibility of the clay stacks, possibly modified by a strongly bound solvent layer. NMR results [19] from suspensions of Claytone in octanol, a system which shows similar platelet alignment in a magnetic field, have confirmed that the solvent remains isotropic in such suspensions. It is therefore reasonable to assume that the elastic constant and magnetic anisotropy of the dodecanol solvent are zero. For concentrations of 0.1% and 1%, there appears to be little orientational interaction between the platelet stacks, since the order parameters are nearly independent of the concentration. However at 10% the ordering is much weaker. This suggests that as concentration increases there are interactions between the platelet stacks that oppose the ordering. Thus we first compare the predictions of the simple model for single-particle ordering outlined above with the order parameters from the more dilute suspensions. Equation (15) predicts a rapid saturation of the order parameter as the field increases, as shown in figure 5 by the fit to the data. The fit is not good for the higher fields,

which suggests that there is some opposition to the ordering from inter-particle interactions as the degree of order becomes high. For this reason the fit has been restricted to the low field data only so that the parameters determined by the fit may be free from this influence.

Typical platelet dimensions are diameter = 500 nm and thickness = 1 nm, and recalling that they are in stacks of ∼4 gives $V = 7.8 \times 10^{-22}$ m^3. Using this value and fitting equation (15) to the low field data gives the anisotropy of the magnetic susceptibility, $\Delta\chi_C = -1.3 \times 10^{-4}$. This is a reasonable magnitude when compared with the $-1.5 \pm 0.5 \times 10^{-4}$ reported for montmorillonite by Wilson [21]. Since montmorillonite is a natural clay and impurity levels depend on the source of the mineral, susceptibility values vary and an exact agreement would not be expected. Furthermore, we have ignored the contribution of strongly bound solvent and the stabilizer. However, we do not believe the latter to be significant, as the magnetic anisotropy of single bonds is small and the pretransitional ordering of the isotropic dodecanol is also small.

A similar alignment of platelets of gibbsite ($Al(OH)_3$) along the magnetic field was observed by Van der Beek *et al* [22]. Converting their results into the units used in the present work, they find $\Delta\chi_C = -2.3 \times 10^{-7}$. The significantly lower value for gibbsite may be a result of the fact that the gibbsite was synthetic, and that therefore impurities such as iron are less likely to be present. Due to the larger particle volume the gibbsite could nevertheless be aligned magnetically. A mineral displaying rather unusual alignment behaviour in magnetic fields is goethite (α-FeOOH) which has a permanent magnetic moment as well as an anisotropic susceptibility $\Delta\chi_C = -3 \times 10^{-4}$ [23]. This allows goethite nanorods to align parallel to the field initially and perpendicular to the field at higher field strength.

4.3. Analysis of order parameters for clay in 5CB

Since the magnetic anisotropy of the clay platelets has been determined in the section above and the physical parameters for nematic 5CB is well known ($\Delta\chi_L = 1.4 \times 10^{-6}$ and $K_3 = 9 \times 10^{-12}$), it is possible to calculate the two terms in equation (14). It becomes $U/(k_BT) = \sin^2\beta[151.2(B/T) - 10.4(B/T)^2]$ and the predicted order parameters, shown in figure 12 saturate at ∼1 for modest fields. The experimental order parameters for the 1% suspension have the correct sign but are much lower than the predicted values. The 1% sample aligned in 4.5 T gave the highest degree of alignment ($\overline{P_2} = 0.35$) and this did not appear to decay while the sample was in zero field. The ESR results on the same system [8] found no evidence for platelet alignment with weaker fields. This suggests that the inter-platelet interactions are stronger in 5CB than they are in dodecanol and that they oppose the alignment by the field, as well as its relaxation when the field is removed.

The absence of any observable alignment for the clay in the isotropic phase of 5CB appears anomalous at first. However, the effective magnetic anisotropy of the platelets is that of the platelet plus any strongly bound solvation layer. In the isotropic phase there are well aligned 5CB molecules between the layers of the stack and on the outer surface the homeotropic alignment will penetrate into the bulk for a distance of about two molecular lengths (∼60 Å just above the transition) [24, 25] due to pretransitional effects. Hence there will be an effective volume of 5CB molecules attached to the platelet stack that is perhaps five times greater than the volume of the clay in the stack. This solvent volume has positive magnetic anisotropy, opposite to the clay platelets. It will certainly reduce and may even reverse the magnetic anisotropy of the stack plus its surrounding of well correlated 5CB molecules. We believe this is the origin of the non-alignment of the clay in isotropic 5CB.

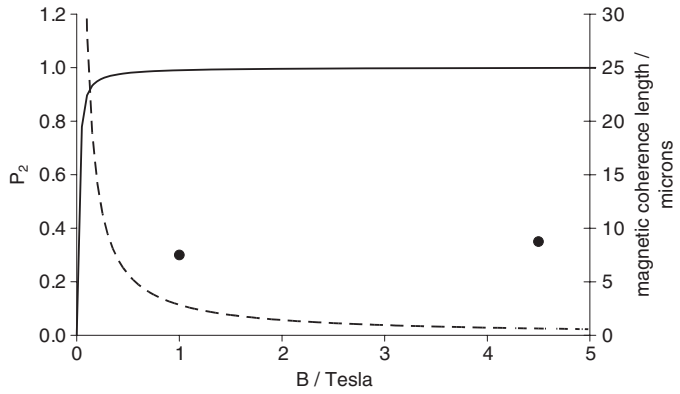

Figure 12. The points are the measured $\overline{P_{2\,\mathrm{CLAY}}}$ for 1% Claytone suspended in 5CB. The solid line is the value of $\overline{P_{2\,\mathrm{CLAY}}}$ expected from the elastic constant and magnetic anisotropy of 5CB and the magnetic anisotropy of the Claytone particles derived from the dodecanol suspensions. The dashed line shows the magnetic coherence length of 5CB.

4.4. Analysis of alignment of 5CB

It was noted that the 5CB peak was only clearly observed for fields above the range 0.4–0.8 T for the 0.2% suspension in 5CB. The magnetic coherence length for 5CB (plotted in figure 12) is about 5 μm in this range. This suggests that there are a substantial number of 5 μm gaps in the composite structure. The typical gap size can only be roughly estimated because the platelet stacks are assembled into loose aggregates. For 0.2% by weight of stacks of four platelets with a spacing of 36 Å dispersed uniformly, a typical gap would be 5 μm but the aggregation would lead to a range of gap sizes. Fields of $\geqslant$1 T would give a coherence length of $\leqslant$3 μm and so most of the volume would be aligned. Fields of $\leqslant$0.4 T would give a coherence length of $\geqslant$7 μm and so most of the volume would be aligned by platelet surfaces rather than the field. This is consistent with the ESR observations where a field of 0.3 T was employed and the alignment appeared to be randomized by the platelets.

The order parameter measured by NMR in the 10% suspension was very similar to that of pure 5CB indicating good director alignment parallel to the field. However, no 5CB peaks were observable using SAXS in zero field from a similar 10% sample cooled in 4.5 T. This too can be understood since the 7 T NMR field will suppress the coherence length to 0.4 μm. Thus if a typical gap between clay stacks is about 2 μm (possible because the effect of higher concentration is offset by the greater degree of large scale aggregation and the increase in stack size to $\sim$15) most of the liquid crystal volume will be aligned with the director parallel to the field. The 4.5 T was sufficient for the director to partly align the platelets ($\overline{P_2} = 0.2$) and this alignment was maintained with the field removed. Since the SAXS pattern was taken in zero field, the coherence length would be 'infinite' and so the director will follow the orientational distribution of the clay platelets. The 5CB peak is therefore distributed broadly and rather little of it satisfies the diffraction conditions. This is illustrated in figure 13.

5. Conclusion

The simple model described above is able to rationalize the opposite alignment of the montmorillonite platelets in dodecanol and nematic 5CB. In the non-mesogenic solvent the magnetic anisotropy of the platelets is the fundamental cause of particle alignment, whereas in

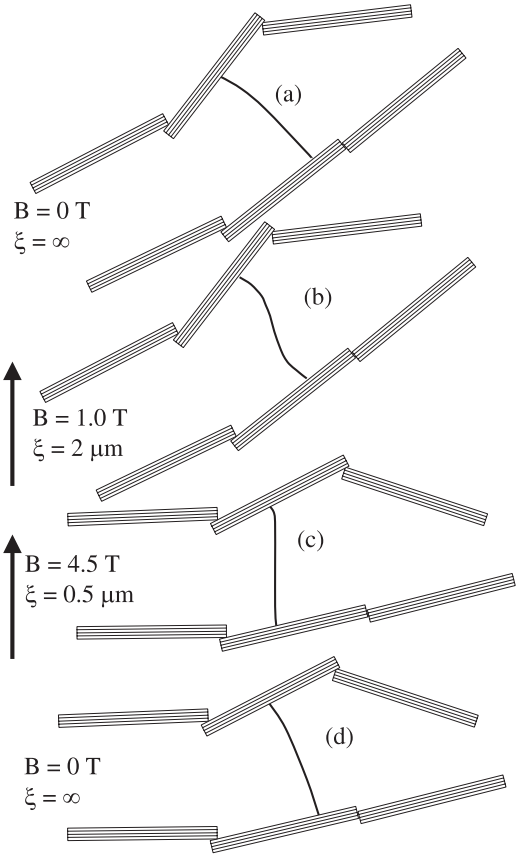

Figure 13. Highly schematic illustration of some platelet stacks and the nearby director in a 10% suspension as a field is applied and removed. The stack and inter-stack gap dimensions are not to scale and variations of stack size are omitted. The platelet stacks are aggregated so there are many different sized gaps, and a typical 2 μm gap is illustrated so that the different stages may be appreciated qualitatively. (a) The initial orientational distribution of platelets is random, and since the magnetic coherence length is infinite in zero field the director is also random. (b) An intermediate field of $1.4 < B/T < 4.5$ is applied, which reduces the magnetic coherence length so some of the liquid crystal has its director parallel to the field but the torque is not sufficient to overcome the friction caused by the aggregation of the platelet stacks. For the lower concentrations (and thus bigger gaps) a substantial fraction of the director becomes aligned at fields below 1.4 T. For instance, the director of a 1% suspension is nearly completely aligned by 1 T as shown in figure 10. (c) A field of 4.5 T is sufficient for the torque to overcome the friction due to the aggregation and some partial alignment of the platelets is achieved. Since the magnetic coherence length is now sub-micron, NMR results indicate the director to be a well aligned monodomain. (d) The field is removed and the platelets remain partly aligned due to their aggregate forming interactions. The magnetic coherence length becomes infinite and so the director distribution becomes broad and resembles that of the platelet normals. Since most of the distribution does not lie along the direction to satisfy the diffraction conditions, there is no observable 5CB peak in the scattering.

the nematic the director aligns with the field and the particles are anchored perpendicular to the director. The model can also qualitatively explain why smaller clay particles such as Laponite do not align in modest magnetic fields. Their particle volume and surface areas are much smaller, and so for 30 nm diameter particles with a similar magnetic anisotropy to Claytone and $B = 1$ T the orientational energy becomes $\sim k_{\mathrm{B}}T$ rather than much larger. For such small platelets in 5CB, $U/(k_{\mathrm{B}}T) = \sin^2\beta[0.55(B/T) - 0.04(B/T)^2]$.

The interactions that oppose the alignment are most probably the same as those that lead to the formation of the large scale aggregates that have been discussed previously [7]. There are different local environments within the open network structure. It is likely that some stacks are relatively free to reorientate, others are become locked as they are rotated by the field and some may be so rigidly held that they are immovable by modest fields. This is clearly a complex system and further experiments will be required to elucidate the nature of the 'frictional' force resulting from the aggregation of the stacks.

Acknowledgments

We would like to thank Geoffrey R Luckhurst, Che R Mamat and Azizah Mainal for sharing generously ESR and NMR results with us and for many stimulating discussions. Without the patient support of Eric Geissler at the ESRF, Grenoble, and Günther Grossmann at the SRS, Daresbury, the SAXS experiments would not have been possible. CP was supported by an IMPACT CASE studentship sponsored by Hewlett Packard and JC was funded via a LINK project.

References

[1] Stark H 2001 *Phys. Rep.* **351** 387–474
[2] Loudet J C, Barois P and Poulin P 2000 *Nature* **407** 611–3
[3] Petrov P G and Terentjev E M 2001 *Langmuir* **17** 2942–9
[4] Glushchenko A, Kresse H, Reshetnyak V, Reznikov Y and Yaroshchuk O 1997 *Liq. Cryst.* **23** 241–6
[5] Kawasumi M, Hasegawa N, Usuki A and Okada A 1996 *Liq. Cryst.* **21** 769–76
[6] Connolly J, van Dvijneveldt J S, Klein S, Pizzey C and Richardson R M 2006 *Langmuir* **22** 6531–8
[7] van Duijneveldt J S, Klein S, Leach E, Pizzey C and Richardson R M 2005 *J. Phys.: Condens. Matter* **17** 2255–67
[8] Luckhurst G R 2006 *Thin Solid Films* **509** 36–48
[9] Kawasumi M, Hasegawa N, Usuki A and Okada A 1999 *Appl. Clay Sci.* **15** 93–108
[10] Pizzey C, Klein S, Leach E, van Duijneveldt J S and Richardson R M 2004 *J. Phys.: Condens. Matter* **16** 2479–95
[11] Confirmed in NMR measurements by Mainal A 2004 private communication
[12] http://www.esrf.fr/expfacilities/BM2/BM2.html
[13] http://srs.dl.ac.uk/info/STATIONINFO/stat21.html
[14] Leadbetter A J, Richardson R M and Colling C N 1975 *J. Physique Coll.* **36** C1 37–43
[15] Chen B and Evans J R G 2006 *Scr. Mater.* **54** 1581–5
[16] Manevitch O L and Rutledge G C 2004 *J. Phys. Chem.* B **108** 1428–35
[17] Weisstein E W *MathWorld—A Wolfram Web Resource* http://mathworld.wolfram.com/SphericalHarmonicAdditionTheorem.html
[18] Warner M 1984 *Mol. Phys.* **54** 677–90
[19] Mainal A 2004 private communication
[20] de Gennes P G and Prost J 1995 *The Physics of Liquid Crystals* (Oxford: Clarendon)
[21] Wilson S R, Ridler P J and Jennings B R 1997 *IEEE Trans. Magn.* **33** 4349
[22] van der Beek D, Petukhov A V, Davidson P, Ferré J, Jamet J P, Wensink H H, Vroege G J, Bras W and Lekkerkerker H N W 2006 *Phys. Rev.* E **73** 041402
[23] Lemaire B J, Davidson P, Ferré J, Jamet J P, Petermann D, Panine P, Dozov I, Stoenescu D and Jolivet J P 2005 *Faraday Discuss.* **128** 271–83
[24] Zink H and de Jeu W H 1985 *Mol. Cryst. Liq. Cryst.* **124** 287
[25] Stinson T W and Lister J D 1973 *Phys. Rev. Lett.* **30** 688